Estimating the foundation parameters of offshore wind turbines through Bayesian model updating

Journal of Physics: Conference Series **2647** (2024) 112008 doi:10.1088/1742-6596/2647/11/112008

Estimating the foundation parameters of offshore wind turbines through Bayesian model updating

H A Simpson[1], K E Tatsis[2], I Abdallah[2], E N Chatzi[2] and M N Chatzis[1]

[1] Department of Engineering Science, University of Oxford, Oxford, UK
[2] Institute of Structural Engineering, Department of Civil, Environmental and Geomatic Engineering, ETH Zürich, Stefano-Franscini-Platz 5, 8093, Zürich, Switzerland

E-mail: henry.simpson@eng.ox.ac.uk

Abstract. The rapid growth of the wind industry has resulted in larger wind turbines with modal properties that lie in the lower frequency range, rendering accurate fatigue assessment increasingly important. However, high uncertainty associated with the support conditions and foundation properties can pose challenges in the condition assessment and fatigue life estimation. One approach to improve these estimates is to use structural monitoring data (e.g. from sensors mounted on the towers) to update the foundation parameters of offshore wind turbine models. However, the low identifiability of the parameters to be estimated can lead to divergent estimates across different frameworks, which, combined with uncertainty in foundation properties, can compromise remaining useful life estimates. In this work, a Bayesian model updating framework is applied to update the foundation parameters of an offshore wind turbine, and its results are compared against a deterministic framework in a numerical example. The advantages of the Bayesian framework over the deterministic framework are discussed in detail and the importance of accurately accounting for uncertainties as part of the model updating process is highlighted.

1. Introduction

The accurate assessment of fatigue life for offshore wind turbines (OWT) often relies on numerical models. However, due to the large uncertainties associated with foundation properties, significant discrepancies may occur between measured and model predicted quantities of interest [1]. To address this, a common strategy is to use in-situ sensor data (such as accelerometers and/or strain gauges) to measure the dynamic response of turbine structures. By applying operational modal analysis (OMA) techniques [2] on ambient vibration data (usually whilst parked, but also during operation [3]), the modal parameters of the structure can be estimated. These can then be compared to the model-estimated modal parameters to calibrate any uncertain parameters. This process is commonly referred to as model updating.

Much of the work related to model updating of large scale infrastructure can be categorised as either deterministic [4–7] or Bayesian [8–12]. The deterministic framework aims to find the optimal set of model parameters that minimise the discrepancy between model outputs and measurements. Beck and Katafygiotis [8] then developed a Bayesian framework that accounts for the uncertainties present when model updating. The Bayesian framework forms a probabilistic model for the uncertain parameters to obtain the *Maxima a Posteriori* (MAP) estimates, i.e., the estimates updated using the data, and their associated uncertainty. This offers the advantage

of evaluating the identifiability of the parameters and assessing the robustness of the model predictions [4].

Both frameworks have been successfully applied to large scale infrastructure such as bridges [10] and buildings [11, 12]. However, the application of these methods for identifying offshore wind turbine foundation properties has received relatively less attention. A deterministic framework has been applied to update the parameters of an OWT jacket foundation in [5] and for monopile foundations in [6, 7]. In [6], the challenges that are unique to the OWT-monopile structure are addressed and the potential for identifying the foundation parameters is demonstrated successfully in a numerical case study. Building upon the contribution in [6], this paper aims to identify the monopile foundation parameters within a Bayesian framework, with the purpose of comparing and demonstrating the advantages of a stochastic approach over deterministic model updating. The paper is structured as follows: a review of the deterministic and Bayesian model updating frameworks is presented in Section 2, followed by a description of the numerical wind turbine model in Section 3. The model is utilized in a numerical case study of a 15 MW OWT to update parameters of the monopile foundation. The generation of synthetic data is discussed in Section 4.1 before the results from the deterministic and Bayesian model updating frameworks are compared in Section 4.2. Finally, conclusions are drawn in Section 5.

2. Model updating framework

2.1. Operational modal analysis

The measured data usually consist of the response due to ambient vibration, recorded using accelerometers or strain gauges. However, OMA techniques [2] are often employed to identify the modal parameters (frequencies and mode shapes) from the measured response. A widely used OMA method is the covariance-driven Stochastic Subspace Identification algorithm, SSI-cov [13]. The algorithm starts by constructing a covariance data matrix from the time history response. Linear algebra techniques are then applied to this data matrix to estimate the state matrix $\hat{\boldsymbol{A}}_d$ and output matrix $\hat{\boldsymbol{C}}$, for a discrete linear time invariant system:

$$\boldsymbol{x}_{k+1} = \hat{\boldsymbol{A}}_d \boldsymbol{x}_k + \boldsymbol{w}_k \quad \& \quad \boldsymbol{y}_k = \hat{\boldsymbol{C}} \boldsymbol{x}_k + \boldsymbol{v}_k, \tag{1}$$

where $\boldsymbol{y}_k$ and $\boldsymbol{x}_k$ are the measurement and state vectors at time step k, respectively. $\boldsymbol{w}_k$ and $\boldsymbol{v}_k$ are the process and measurement noise, which are unknown but assumed to have a zero-mean discrete white noise structure. The notation $\hat{}$ is used to represent an identified parameter and distinguish it from model-estimated parameters defined later. Once $\hat{\boldsymbol{A}}_d$ has been estimated, it is then converted to its continuous form through: $\hat{\boldsymbol{A}}_c = \log\left(\hat{\boldsymbol{A}}_d\right)/dt$, where dt is the sampling time step and log denotes the matrix logarithm. The modal parameters can then be extracted from an eigenvalue analysis on the state space matrix $\hat{\boldsymbol{A}}_c$:

$$\hat{\boldsymbol{A}}_c \hat{\boldsymbol{\Psi}} = \hat{\boldsymbol{\Psi}} \hat{\boldsymbol{\Lambda}}, \tag{2}$$

where $\hat{\boldsymbol{\Lambda}}$ is the diagonal eigenvalue matrix and $\hat{\boldsymbol{\Psi}}$ is the eigenvector matrix.

The diagonal terms in $\hat{\boldsymbol{\Lambda}}$ contain the eigenvalues $\hat{\lambda}_i$, from which the ith natural frequency in Hz $\hat{f}_i$ can be calculated:

$$\hat{f}_i = \frac{|\hat{\lambda}_i|}{2\pi}, \tag{3}$$

$\hat{\boldsymbol{\Psi}}$ contains the corresponding eigenvectors, which can be combined with $\hat{\boldsymbol{C}}$ to yield the mode shape matrix $\hat{\boldsymbol{\Phi}}$ in the sensor basis:

$$\hat{\boldsymbol{\Phi}} = \hat{\boldsymbol{C}} \hat{\boldsymbol{\Psi}}. \tag{4}$$

2.2. Deterministic model updating

The deterministic approach to formulating such a framework consists of an objective function $J(\boldsymbol{\theta})$, which evaluates discrepancies between the model predictions and the measured data. Once OMA has been carried out on the vibration data, the objective function can be defined based on the modal parameters. A commonly used metric to compare two mode shapes, $\boldsymbol{\phi}_1$ and $\boldsymbol{\phi}_2$, is the modal assurance criterion (MAC) [14], which is also known as the cosine similarity metric:

$$\mathrm{MAC}(\boldsymbol{\phi}_1, \boldsymbol{\phi}_2) = \frac{|\boldsymbol{\phi}_1 \boldsymbol{\phi}_2^*|^2}{\boldsymbol{\phi}_1 \boldsymbol{\phi}_1^* \boldsymbol{\phi}_2 \boldsymbol{\phi}_2^*}, \tag{5}$$

where $(\cdot)^*$ indicates the (complex conjugate) transpose of a vector. The MAC takes a value between zero and one, where a MAC of one indicates that two vectors are colinear and a MAC of zero indicates that two vectors are orthogonal.

In this work, the objective function is defined as:

$$J(\boldsymbol{\theta}) = \sum_{i=1}^{N_m} \left(\frac{f_i(\boldsymbol{\theta}) - \hat{f}_i}{\hat{f}_i} \right)^2 + \sum_{i=1}^{N_m} \left(1 - \mathrm{MAC}(\boldsymbol{\phi}_i(\boldsymbol{\theta}), \hat{\boldsymbol{\phi}}_i) \right), \tag{6}$$

where $f_i(\boldsymbol{\theta})$ and $\boldsymbol{\phi}_i(\boldsymbol{\theta})$ are the ith model predicted frequency and mode shape respectively, for a chosen realization of the parameters $\boldsymbol{\theta}$. $\hat{f}_i$ and $\hat{\boldsymbol{\phi}}_i$ are the ith identified frequency and mode shape. N_m is the total number of modes identified from the data.

The updated parameter estimates $\boldsymbol{\theta}^{opt}$ are those which minimise the objective function $J(\boldsymbol{\theta})$:

$$\boldsymbol{\theta}^{opt} = \arg\min_{\boldsymbol{\theta}} J(\boldsymbol{\theta}). \tag{7}$$

2.3. Bayesian Model Updating

Beck and Katafygiotis [8] were among the first to use a Bayesian model updating framework for civil structures. This probabilistic framework utilises prior information and updates it as new data become available, resulting in a posterior distribution for the uncertain parameters. Equation 8 presents this mathematically, where $\boldsymbol{\theta}$ is a set of uncertain model parameters from the joint model class, $\mathcal{M}$, and $\hat{\boldsymbol{d}}$ is the measured data.

$$p(\boldsymbol{\theta}|\hat{\boldsymbol{d}}, \mathcal{M}) = \frac{p(\hat{\boldsymbol{d}}|\boldsymbol{\theta}, \mathcal{M}) p(\boldsymbol{\theta}|\mathcal{M})}{p(\hat{\boldsymbol{d}}|\mathcal{M})}. \tag{8}$$

In Equation 8, $p(\boldsymbol{\theta}|\hat{\boldsymbol{d}}, \mathcal{M})$ is the posterior distribution, $p(\hat{\boldsymbol{d}}|\boldsymbol{\theta}, \mathcal{M})$ is the likelihood, $p(\boldsymbol{\theta}|\mathcal{M})$ is the prior distribution and $p(\hat{\boldsymbol{d}}|\mathcal{M})$ is the evidence.

For a fixed model class and given data set, $p(\hat{\boldsymbol{d}}|\mathcal{M})$ is independent of $\boldsymbol{\theta}$ and can be considered as a constant which ensures that the posterior probability density function (PDF) integrates to one.

$p(\boldsymbol{\theta}|\mathcal{M})$ takes into account any previously acquired knowledge about the uncertain parameters $\boldsymbol{\theta}$, before measurements have been observed. The prior is often chosen based on expertise or engineering judgement. Common approaches for selecting $p(\boldsymbol{\theta}|\mathcal{M})$ include the use of the principle of Maximum Entropy [12] or conjugate priors [15].

$p(\hat{\boldsymbol{d}}|\boldsymbol{\theta}, \mathcal{M})$ is used to determine how well the measured data agree with the model predictions and can be considered as the Bayesian counterpart to the deterministic objective function. To formulate $p(\hat{\boldsymbol{d}}|\boldsymbol{\theta}, \mathcal{M})$, a probabilistic model must be assumed to represent the prediction error between the model outputs and the measurements. Similarly to the deterministic objective

function, the prediction error can defined in terms of the modal data. In this work, the following prediction error vector was considered: $\boldsymbol{\eta} = \{\boldsymbol{\eta_f}; \boldsymbol{\eta_\phi}\} \in \mathbb{R}^{N_m(N_o+1)}$.

$$\boldsymbol{\eta_f} = \boldsymbol{f}(\boldsymbol{\theta}) - \hat{\boldsymbol{f}} \in \mathbb{R}^{N_m} \quad \& \quad \boldsymbol{\eta_\phi} = \boldsymbol{\phi}(\boldsymbol{\theta}) - \hat{\boldsymbol{\phi}} \in \mathbb{R}^{N_m N_o}.$$

N_m is the number of modes and N_o is the number of mode shape components.

The probabilistic model for the prediction error is commonly assumed to be a Gaussian distribution with zero mean so that the likelihood function can be defined as:

$$p(\hat{\boldsymbol{d}}|\boldsymbol{\theta}, \mathcal{M}) \propto \det(\boldsymbol{\Sigma})^{-1/2} \exp(-\frac{1}{2}\boldsymbol{\eta}^T \boldsymbol{\Sigma} \boldsymbol{\eta}). \tag{9}$$

In this work, it is assumed that $\boldsymbol{\Sigma} = \boldsymbol{\Sigma}_G + \boldsymbol{\Sigma}_D$, where $\boldsymbol{\Sigma}_G$ and $\boldsymbol{\Sigma}_D$ are the model and measurement covariance matrices, respectively. Furthermore, all frequencies and mode shape components are assumed to be uncorrelated so that that $\boldsymbol{\Sigma}$ is a diagonal matrix. Although this formulation accounts for both measurement and modelling uncertainties, it can be viewed as a limitation of the framework to group them together. This is because only the total error can be identified, making it difficult to differentiate between the two types of uncertainty [12].

The SSI-cov algorithm has been extended in [13] to estimate the uncertainty associated with the identified frequencies and mode shapes: $\text{Cov}\left(\hat{f}_i\right)$ and $\text{Cov}\left(\hat{\boldsymbol{\phi}}_i\right)$. In this work, these covariances were utilised to define the diagonal terms of $\boldsymbol{\Sigma}_D$.

$\boldsymbol{\Sigma}_G$ is defined by a set of parameters $\boldsymbol{\theta}_G$, which are updated alongside the structural parameters $\boldsymbol{\theta}_M$, so that the set of probabilistic model parameters to be updated becomes $\boldsymbol{\theta} = \{\boldsymbol{\theta}_M; \boldsymbol{\theta}_G\}$. The standard deviation for the ith frequency and mode shape is assumed to be proportional to the ith identified frequency $\hat{f}_i$ and mode shape $\hat{\boldsymbol{\phi}}_i$:

$$\sigma_{f,i} = \sigma_f \hat{f}_i \quad \& \quad \sigma_{\boldsymbol{\phi},i} = \sigma_{\boldsymbol{\phi}} \|\hat{\boldsymbol{\phi}}_i\| \tag{10}$$

where σ_f and $\sigma_{\boldsymbol{\phi}}$ are unknown dimensionless parameters to be updated. The model frequency and mode shape variances, $\sigma^2_{f,i}$ and $\sigma^2_{\boldsymbol{\phi},i}$, are then set to the corresponding diagonal entries in $\boldsymbol{\Sigma}_G$. In order to keep the number of updating parameters to a minimum, σ_f and σ_ϕ are assumed to be equal (i.e., $\sigma = \sigma_f = \sigma_\phi$).

Evaluating $p(\boldsymbol{\theta}|\hat{\boldsymbol{d}}, \mathcal{M})$ typically involves solving complex high-dimensional integrals. Therefore, a common approach to compute the posterior is to use sampling methods, such as Markov Chain Monte Carlo (MCMC) methods, nested sampling, or Transitional MCMC (TMCMC) [16, 17].

Mode shape normalisation

It is shown in [6], that when the normalisation scheme presented by Fillod [18], termed *complex normalisation*, is applied to a damped mode shape (whether proportionally or non-proportionally damped), the result is a good approximation of the corresponding undamped mode shape. Therefore, in this work, complex normalisation (Equation 11) is applied to compare the mode shapes:

$$\bar{\boldsymbol{\phi}}^C = Re\left(\frac{\boldsymbol{\phi}_d}{\phi_{d,i}}\right), \tag{11}$$

where $\bar{\boldsymbol{\phi}}^C$ is the complex normalised mode shape, which approximates the damped mode shape $\boldsymbol{\phi}_d$. The index, i, corresponds to the mode shape component that maximises $|\phi_{d,i}|$.

3. Simscape wind turbine model

In this section, an overview of the OWT model is described. The coupled hydro-aero-elastic model was developed in Matlab/Simulink and is based on the IEA Wind 15-MW reference turbine [19] with a monopile foundation. In Section 4 this model is used for both synthetic data generation and for updating the foundation parameters of a parked OWT.

3.1. Tower, monopile and blade modelling

The tower and monopile are modelled using ten uniform cylindrical Euler-Bernoulli beam elements each. Figure 1 shows the main dimensions of the wind turbine model. Both the monopile and tower are made from steel with elastic modulus and Poisson's ratio equal to 210 GPa and 0.3 respectively. The monopile extends from ground level to 15 m above the mean water level with density 7850 kg/m^3. The tower then sits on top of the monopile and extends to 145 m above the mean water level with density 8500 kg/m^3. The diameter and wall thickness distributions can be found in the reference document [19].

The blades are also modelled using beam elements. Due to their complex shape, the flexible beam elements are defined by reduced order mass and stiffness matrices. Based on the blade mass, stiffness and inertia distributions defined in [19], Euler-Bernoulli beam theory was used to assemble the full stiffness and mass matrices for each blade element. Craig-Bampton reduction [20] was then applied to obtain the reduced order mass and stiffness matrices with two modes retained per element. Each blade had a total of six reduced order elements.

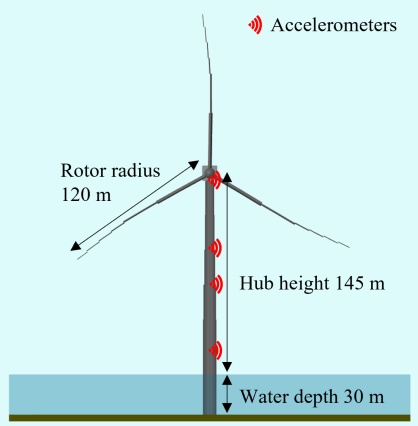

Figure 1. Overview of 15 MW offshore wind turbine with tower accelerometers.

$$\begin{bmatrix} H_G \\ M_G \end{bmatrix} = \begin{bmatrix} k_{11} & k_{12} \\ k_{12} & k_{22} \end{bmatrix} \begin{bmatrix} v_g \\ \psi_g \end{bmatrix}$$

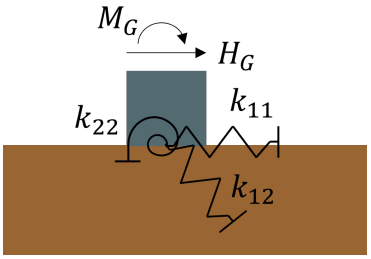

Figure 2. Coupled springs foundation representation. v_g and ψ_g are the ground level displacement and rotation, respectively.

3.2. Foundation modelling

The foundation is modelled using a linear elastic coupled spring foundation, which consists of translational k_{11}, rotational k_{22} and cross-coupling k_{12} springs, as shown in Figure 2.

In Section 4, the three coupled spring stiffness constants are considered as uncertain model parameters and are updated within the frameworks described in Section 2. However, to generate synthetic data for a numerical case study, the following baseline stiffness matrix $\boldsymbol{K}_0$ was defined:

$$\boldsymbol{K}_0 = \begin{bmatrix} 0.098 & 0.678 \\ 0.678 & 8.238 \end{bmatrix} \times 10^{11} \text{ N/m}. \tag{12}$$

3.3. Calculation of the model estimated modal parameters

To calculate the modal parameters, the Simulink model is linearised about a steady-state operating point to generate a continuous-time state-space model:

$$\dot{\boldsymbol{x}} = \boldsymbol{A}|_{op}\,\boldsymbol{x} + \boldsymbol{B}|_{op}\,\boldsymbol{u}, \quad \& \quad \boldsymbol{y} = \boldsymbol{C}|_{op}\,\boldsymbol{x} + \boldsymbol{D}|_{op}\,\boldsymbol{u}, \tag{13}$$

where $\boldsymbol{x}$ is the state vector, $\boldsymbol{u}$ is the input vector, $\boldsymbol{y}$ is the output vector, and $\dot{}$ indicates a time derivative. The matrices $\boldsymbol{A}|_{op}$, $\boldsymbol{B}|_{op}$, $\boldsymbol{C}|_{op}$, $\boldsymbol{D}|_{op}$, represent the state, input-state, output

and feed-through matrices, respectively. The subscript *op* indicates that these matrices are evaluated with respect to a specific operating point. Once $\boldsymbol{A}|_{op}$ and $\boldsymbol{C}|_{op}$ have been obtained, the model-estimated modal parameters can be calculated using Eqs. 2-4.

4. Numerical example: application to a parked 15 MW wind turbine

In this section, the two model updating frameworks described in Section 2 are applied to update the uncertain coupled spring foundation parameters using the model outlined in Section 3. First the generation of synthetic data is discussed before presenting the results from OMA and model updating.

4.1. Synthetic data generation and OMA results

Synthetic data was generated with the foundation stiffness set to $\boldsymbol{K}_0$ and the turbine in a parked configuration, i.e., locked rotor and blades pitched to 90 degrees. A turbulent wind field was generated using Turbsim [21] and then applied to the Simscape model, defined by a mean wind speed at hub height equal to 2 m/s and a turbulent intensity of 10%. Additionally, unidirectional wave loading was applied which was calculated based on a JONSWAP spectrum [22] with significant wave height, $H_s = 3.5\,\text{m}$, and peak wave period $T_p = 8\,\text{s}$. The wind and waves were assumed to be aligned and applied in the fore-aft direction (i.e. yaw angle equal to zero).

Simulations were run for 750 seconds with the first 150 seconds discarded to remove any transient effects, resulting in a ten minute data set. Four bi-axial accelerometers in the fore-aft (FA) and side-side (SS) directions were used to measure the response along the wind turbine tower, as shown in Figure 1. Then to replicate the noise that exists in practical sensors, the acceleration time histories were corrupted by random Gaussian noise with a standard deviation equal to 3% of the RMS value of each signal.

For a reasonable comparison between the identified and model estimated modal parameters, the model should be linearised about an operating point that is representative of the conditions for which the data is recorded. Therefore, the model estimated modal parameters were calculated about the steady state operating point corresponding to a constant 2 m/s wind field in still water.

OMA was carried out on the eight acceleration signals using SSI-cov, to identify the modal parameters. Table 1 lists the frequencies of the identified modes and compares them with the corresponding model frequencies evaluated at $\boldsymbol{K}_0$. It can be seen that there is minimal error between the model estimated and identified frequencies. Table 1 also provides a comparison between the model and identified mode shapes using the MAC values (Equation 5). From Table 1, all modes apart from 1 and 4 have MAC values close to one, indicating that the mode shapes have been accurately identified. However, for modes 1 and 4, which correspond to the only side-side tower modes, the MAC values are much lower, suggesting poor identification of these mode shapes. This is a practical issue related to applying system identification methods to quasi-axisymmetric structures, such as OWTs and has been discussed in detail in [6]. It should be noted that although these mode shapes have been poorly identified, the associated uncertainty estimated using SSI-cov is higher for these modes than the accurately identified modes. This is taken into account within in the Bayesian framework but not in the deterministic approach.

4.2. Model updating results

In this section, the results from application of both the deterministic and Bayesian model updating frameworks are presented. The model from Section 3, is used to estimate the properties of the coupled spring foundation parameters: $\boldsymbol{\theta}_M = \{k_{11}; k_{22}; k_{12}\}$.

The deterministic problem was solved using MATLAB's fminsearch optimisation algorithm [23], to minimise the objective function shown in Equation 6. The optimisation algorithm requires an initial starting point $\boldsymbol{K}_{init}$. In order to explore the impact of the initial search point, three initial values were considered, defined by a scalar γ_{init}, where $\boldsymbol{K}_{init} = \gamma_{init}\boldsymbol{K}_0$.

Table 1. Comparison between identified and model modes evaluated at $\boldsymbol{K}_0$. SS refers to a side-side tower mode and FA refers to a fore-aft tower mode.

Mode No.	Dominant tower direction	Model frequency [Hz]	Identified frequency [Hz]	Relative frequency error [%]	MAC [-]
1	SS	0.1573	0.1567	0.37	0.038
2	FA	0.1587	0.1586	0.11	0.999
3	FA	0.6284	0.6279	0.08	1.000
4	SS	1.0898	1.0890	0.08	0.309
5	FA	1.1064	1.1054	0.09	1.000
6	FA	1.8298	1.8257	0.22	0.988
7	FA	2.5729	2.5854	0.48	0.998
8	FA	3.8598	3.8637	0.10	1.000
9	FA	5.7920	5.7667	0.44	0.999
10	FA	10.2769	10.2588	0.18	1.000
11	FA	12.1961	12.2060	0.08	0.996

The Bayesian posterior distributions were obtained by generating 100 000 samples using the TMCMC algorithm. The likelihood was defined using Equations 9-10. Uniform priors were assumed for all updating parameters, where the structural parameters (k_{11}, k_{22}, k_{12}) are bounded between 0.25 and 4 times their nominal values. The model uncertainty parameter σ is bounded between 0 and 0.1.

Deterministic vs Bayesian model updating

Table 2 shows the optimal deterministic estimates $\boldsymbol{\theta}^{opt}$, as well as the MAP estimates $\boldsymbol{\theta}^{\text{MAP}}$ from the Bayesian framework. Associated with each deterministic estimate is the objective function value $J(\boldsymbol{\theta}^{opt})$. Comparing $\boldsymbol{\theta}^{opt}$ against $\boldsymbol{\theta}^{\text{MAP}}$ reveals that the Bayesian estimates are closer to the true parameter values than the deterministic results. Figure 3 shows the updated posterior distribution for the foundation parameters and the model uncertainty parameter σ. The narrow posterior distributions centered close to the true parameter values indicate the identifiability of the foundation parameters for this case. Moreover, the joint posterior distributions in Figure 3 allow for the assessment of the parameter correlation. The results show a strong positive correlation between each of the foundation parameters, as expected. In contrast, it is difficult to assess the identifiability of the deterministic results since the parameter uncertainty is not quantified.

To assess the robustness of the deterministic results, the optimisation algorithm was repeated with various initial values to check for consistent estimates of $\boldsymbol{\theta}^{opt}$. Table 2 presents the results for three different values of γ_{init}, which indicate that depending on γ_{init}, different optimal parameter estimates are obtained. This implies that the objective function comprises multiple peaks. By comparing the objective function value at the optimal parameter estimates $J(\boldsymbol{\theta}^{opt})$, the solution using $\gamma_{init} = 1$ tends to yield the global minimum, whereas local minima were obtained otherwise. While the global minimum produces the most accurate (deterministic) parameter estimates for this example, due to modelling and identification errors, this may not be the case generally and makes it difficult to trust the deterministic results. On the other hand, Figure 3 shows that the Bayesian framework results in a posterior distribution with a single peak. This observation can be attributed to two factors. Firstly, unlike the deterministic approach that uses the MAC to compare mode shapes in the objective function, the Bayesian approach compares each mode shape component individually in a vector-based approach and

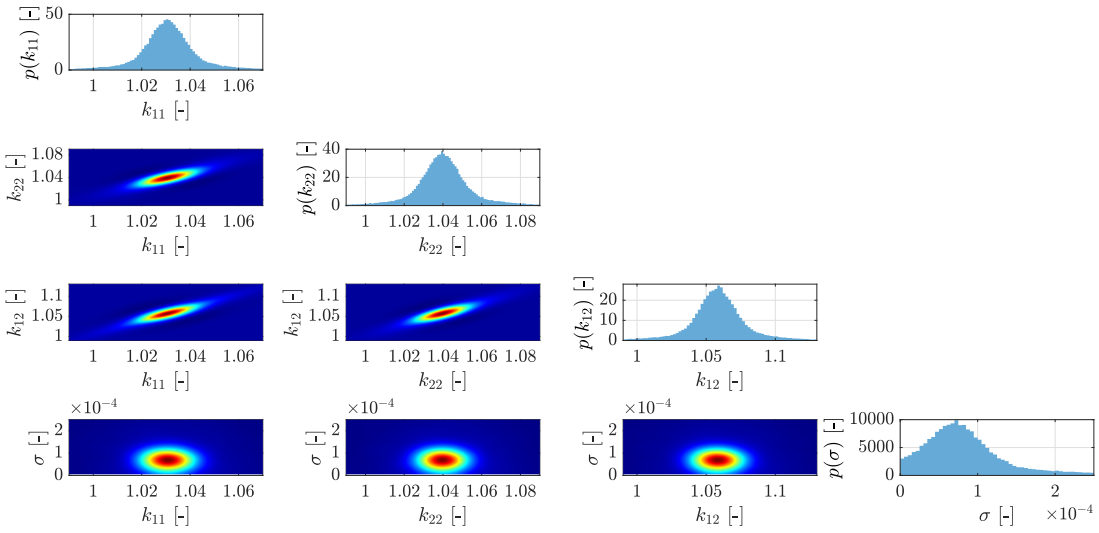

Figure 3. Posterior distributions for the foundation parameters (k_{11}, k_{22}, k_{12}) and model uncertainty parameter (σ). k_{11}, k_{22} and k_{12} have been normalised by their true values.

also assumes a Gaussian likelihood function. Secondly, due to the measurement uncertainty in the Bayesian framework, less weight is assigned to the poorly identified modes, thus reducing their influence on the results. In contrast, the deterministic approach assigns the same weight to all modes.

Finally, the Bayesian framework allows for quantification of the joint model uncertainty through updating the parameter σ. The joint model uncertainty reflects the combined error in the numerical model and the probabilistic model for the prediction error. In this case, the same numerical model is used for both synthetic data generation and model updating. Therefore, since there is no error in the OWT model, σ should only reflect the uncertainty in the probabilistic model for the prediction error. Table 2 and Figure 3 show that the updated distribution for σ is extremely low. A low value for σ indicates that the measurement uncertainty is accurately estimated from SSI-cov and the modelling error is negligible, as expected.

Table 2. Updated deterministic and Bayesian parameter estimates. Deterministic results corresponding to the global minimum of the objective function $J(\boldsymbol{\theta}^{opt})$ are shown in bold.

Deterministic results					**Bayesian results**			
γ_{init} [-]	$\boldsymbol{\theta}^{opt}$ Percentage errors			$J(\boldsymbol{\theta}^{opt})$ [-]	$\boldsymbol{\theta}^{\text{MAP}}$ Percentage errors			σ [-]
	k_{11} [%]	k_{22} [%]	k_{12} [%]		k_{11} [%]	k_{22} [%]	k_{12} [%]	
0.25	5.91	-47.6	-16.7	2.027				
1	**-8.84**	**11.32**	**-7.09**	**1.66**	2.83	3.9	5.42	3.24×10^{-6}
4	222.79	336.52	366.4	1.84				

5. Conclusions

This work compares deterministic and Bayesian model updating methods for identifying the coupled spring foundation parameters of the IEA-15MW reference turbine in a numerical example. The deterministic objective function in [6] was used and the results were compared to a Bayesian framework that has been widely applied to bridge and building structures but has not

yet been applied to identify OWT foundations. Based on the results, the following conclusions were drawn.

The Bayesian MAP estimates were closer to the true parameter values and more identifiable than the deterministic estimates. This was attributed to the Bayesian approach comparing mode shape components, assigning less weight to poorly identified modes, and allowing for quantification of model uncertainty through the parameter σ.

The posterior probability distributions obtained from the Bayesian framework were used to assess the identifiability and the correlation of the parameters. In contrast, the identifiability of the deterministic results was difficult to assess and the significantly different optimal parameter estimates obtained from varying the initial search point highlights the challenges associated with the deterministic method.

Overall, the results demonstrate several advantages of the Bayesian framework over the deterministic approach. The results discussed in this work were based on a numerical case study which does not consider any modelling bias. Therefore, future research will investigate the impact of modelling errors on the identifiability of the foundation parameters.

6. Acknowledgements

This research was financially supported by RWE Renewables. The authors would like to acknowledge the support of Professor Costas Papadimitriou for his suggestions and Dr Xinyu Jia for sharing the code for TMCMC sampling.

References

[1] Kallehave D, Byrne B W, LeBlanc Thilsted C and Mikkelsen K K 2015 *Philosophical Transactions of the Royal Society A: Mathematical, Physical and Engineering Sciences* **373** 20140100
[2] Reynders E 2012 *Archives of Computational Methods in Engineering* **19** 51–124
[3] Avendano-Valencia L D, Chatzi E N and Tcherniak D 2020 *Mechanical Systems and Signal Processing* **142** 106686
[4] Simoen E, De Roeck G and Lombaert G 2015 *Mechanical Systems and Signal Processing* **56** 123–149
[5] Augustyn D, Smolka U, Tygesen U T, Ulriksen M D and Sørensen J D 2020 *Applied Ocean Research* **104** 102366
[6] Anderson E F 2022 *Identification of Offshore Wind Turbine Foundation Properties from Monitoring Data* Ph.D. thesis University of Oxford
[7] Henkel M 2022 *Validation of virtual sensing for the fatigue assessment of subsoil and submerged components of offshore wind turbines* Ph.D. thesis Vrije Universiteit Brussel
[8] Beck J and Katafygiotis L 1998 *I-Baysian Statistical Framework*
[9] Simoen E, Papadimitriou C and Lombaert G 2013 *Journal of Sound and Vibration* **332** 4136–4152
[10] Argyris C, Papadimitriou C, Panetsos P and Tsopelas P 2020 *Journal of Sensor and Actuator Networks* **9** 27
[11] Behmanesh I, Moaveni B, Lombaert G and Papadimitriou C 2015 *Mechanical Systems and Signal Processing* **64** 360–376
[12] Simoen E, Moaveni B, Conte J P and Lombaert G 2013 *Journal of Engineering Mechanics* **139** 1818–1830
[13] Reynders E, Pintelon R and De Roeck G 2008 *Mechanical systems and signal processing* **22** 948–969
[14] Allemang R J 1982 A correlation coefficient for modal vector analysis *Proc. of the 1st IMAC* pp 110–116
[15] Song M, Behmanesh I, Moaveni B and Papadimitriou C 2020 *Sensors* **20** 3874
[16] Lye A, Cicirello A and Patelli E 2021 *Mechanical Systems and Signal Processing* **159** 107760
[17] Ching J and Chen Y C 2007 *Journal of engineering mechanics* **133** 816–832
[18] Fillod R 1980 *Doctor of Sciences Physics Dissertation, University of Besançon, France*
[19] Gaertner E, Rinker J, Sethuraman L, Zahle F, Anderson B, Barter G E, Abbas N J, Meng F, Bortolotti P, Skrzypinski W *et al.* 2020 Iea wind tcp task 37: definition of the iea 15-megawatt offshore reference wind turbine Tech. rep. National Renewable Energy Lab.(NREL), Golden, CO (United States)
[20] Craig Jr R R and Bampton M C 1968 *AIAA journal* **6** 1313–1319
[21] Jonkman B and Kilcher L 2012 *National Renewable Energy Laboratory: Golden, CO, USA*
[22] Hasselmann K, Barnett T P, Bouws E, Carlson H, Cartwright D E, Enke K, Ewing J, Gienapp A, Hasselmann D, Kruseman P *et al.* 1973 *Ergaenzungsheft zur Deutschen Hydrographischen Zeitschrift, Reihe A*
[23] Lagarias J C, Reeds J A, Wright M H and Wright P E 1998 *SIAM Journal on optimization* **9** 112–147